Physicochemical Characterization of Carrageenans—A Critical Reinvestigation

Gisela Berth,[1] Jasna Vukovic,[2] M. Dieter Lechner[2]

[1]*Polymer Consultant Office, In den Gehren 2, D-14558 Nuthetal, Germany*
[2]*Institute of Physical Chemistry, University of Osnabrueck, D-49069 Osnabrueck, Germany*

Received 23 January 2008; accepted 9 June 2008
DOI 10.1002/app.28937
Published online 15 September 2008 in Wiley InterScience (www.interscience.wiley.com).

ABSTRACT: Kappa-, iota-, and lambda-carrageenan (food grade) were analyzed by static light scattering (MALS in batch mode) in 0.1*M* $NaNO_3$ at 25 and 60°C, earlier heated up to 90°C or not. At 25°C, there was a strong tendency for a concentration-dependent aggregation in the order lambda < kappa < iota. At 60°C, all samples were molecularly dispersed. The strongly temperature-dependent refractive index increments (equilibrium dialysis) differ. Data interpretation in terms of the wormlike chain model using the Skolnik-Odijk-Fixman approach led to an intrinsic persistence length around 3 to 4 nm and expansion factors as high as 1.5 and above in a thermodynamically good solvent for all three types. Triple-detector HPSEC (DRI, MALS, viscometry) on the three commercial samples plus a degraded (by acidic hydrolysis) kappa-carrageenan in the same solvent/eluant at 60°C yielded a uniform and slightly curved $[\eta]$-*M* relationship for $5 \times 10^3 \leq M/(\text{g mol}) \leq 3 \times 10^6$ and a nearly identical molar mass dependence of the radius of gyration. HPSEC at 25°C on kappa-carrageenan confirmed formation of soluble aggregates. Special emphasis was put on analytical and methodological aspects. The reliability of the experimental data was demonstrated by analogous measurements on dextran calibration standards. © 2008 Wiley Periodicals, Inc. J Appl Polym Sci 110: 3508–3524, 2008

Key words: biopolymers; static light scattering; gel permeation chromatography light scattering; solution properties water-soluble polymers; temperature effects

INTRODUCTION

The term "carrageenan" refers to a group of sulfated galactans, which are extracted on a commercial scale from various red seaweeds. Carrageenans are mainly used as food additives. Idealized formulae describe the repeating unit of kappa-carrageenan as (1,3-linked) D-galactose-4-sulfate and (1,4-linked) 3,6-anhydro-D-galactose. The repeating unit of iota-carrageenan contains an additional sulfate at the second carbon of the 3,6-anhydro-D-galactose unit. Kappa- and iota-carrageenan share the same backbone which makes them close relatives. Lambda-carrageenan is also composed of a disaccharide repeating unit but this consists of (1,3-linked) D-galactose-2-sulfate and (1,4-linked) D-galactose-2,6-disulfate. Consequently, all three carrageenan types can be classified as linear chains and strong polyelectrolytes.

Like other polysaccharides, carrageenans are polydisperse (at least) with respect to their molar mass. The molar mass distribution varies from lot to lot.

Correspondence to: G. Berth (gberth@t-online.de).

The physicochemical characterization by static light scattering [standing alone or in combination with size exclusion chromatography (SEC)] has been the subject of many publications[1–19] during the last 30 years. An incomplete but representative reference list is given later. Many of these studies aimed at finding experimental evidence for a conformation transition (helix-coil) of kappa- and iota-carrageenans parallel to the changes in the optical activity as a function of temperature or sort and concentration of added salt. (The transition temperature normally lies somewhere between 45 and 50°C.) These studies suggest a strong tendency for association in the "ordered" or helical conformation that interferes with the molecular characterization. This is a complicated situation, indeed, and the typical difficulties of light scattering measurements in aggregating systems might partly explain the diversity of findings regarding the conformation in the ordered state.

Kappa-carrageenan in the "disordered" state appears to be the best-characterized member of the family. There is general agreement on its coil-like conformation. Based on static light scattering and hydrodynamic measurements, Vreeman et al.[1] concluded on relatively flexible and partly drained chains, which was later supported by findings from elsewhere.[3] The intrinsic persistence lengths in 0.1*M*

NaCl at room temperature were calculated to be 7.8 and 6.8 nm.[1,3]

Big parts of the confusion in the literature may result from unsolved or undiscovered methodological problems and/or an uncritical use of data. Often missing experimental details aggravate the situation for the skilled reader by making any scrutiny impossible. This involves the used refractive index increments. Occasionally, data from other groups were adopted unproven or were verified in a nontransparent manner.[19]

Therefore, faced with the characterization of carrageenans by light scattering in terms of average molar mass, molar mass distribution, and, eventually, chain conformation, we would not imitate any published approach but develop our own procedure as we used to do on other complex (ionic) polysaccharides.[20,21] This includes measuring the refractive index increments. Again, we would apply static light scattering standing alone as the method of choice for studying the unfractionated parent samples. According to the cited literature, temperature affects both the solubility of carrageenans and the solute's behavior in solution. Therefore, we would prepare the solutions at various temperatures and perform the measurements at temperatures well above and well below the transition temperature. We would follow Ref. 7 by taking 0.1*M* $NaNO_3$ as solvent and eluant in SEC. An ionic strength of 0.1*M* was supposed to be suitable to properly suppress all kinds of polyelectrolyte effects, see Refs. 20 and 21.

Having discovered suitable conditions for preparing and studying molecularly dispersed solutions, we would combine size exclusion chromatography (HPSEC) with (on-line) multi-angle light scattering (MALS) and viscosity measurements in the eluant to get information on the molar mass distribution along with the molar mass dependence of the radius of gyration and the intrinsic viscosity, respectively.

Thus obtained results are the subject of this report and the focus is on analytical and methodological aspects. Emphasis is put on issues as they may arise from measurements at various temperatures. This means not only temperature-dependent optical parameters such as the refractive index increment and refractive index of the solvent (light scattering) but also the possibly temperature-dependent calibration of the used equipment (light scattering photometer, differential refractometer at HPSEC). Another point is the critical evaluation of triple-detector HPSEC data. To check the correctness of our data, we tested our equipments by means of dextran calibration standards. Dextrans were chosen for their uncomplicated behavior under changing conditions. The three used commercial carrageenan samples were taken to be representative model substances.

EXPERIMENTAL

Materials and preparation of solutions

The three commercial food-grade carrageenans (Kelco) as well as the two dextran calibration standards having average molar masses of $M_w = 4 \times 10^4$ g mol^{-1} and 5×10^6 g mol^{-1} were delivered from the Wyatt Technology Corporation (Santa Barbara, CA). Kappa-carrageenan was also degraded for 30 min in hot sulfuric acid,[22] and the subsequently neutralized (by adding aqueous sodium hydroxide) solution was then analyzed by HPSEC.

0.1*M* $NaNO_3$ containing sodium azide ($\sim$ 20 mg L^{-1}) for preservation was used as solvent and eluant upon batch-mode MALS and HPSEC. The weighed amount of the polysaccharide sample was dispersed overnight at room temperature to give solutions with $\sim$ 3 mg mL^{-1} at the utmost (apart from the degraded kappa-carrageenan and dextran of 4×10^4 g mol^{-1}). Thus, obtained carrageenan dispersions were kept for 10 min at 90°C (water bath) under slight shaking and were then cooled to the specified measuring temperature, i.e., 25 and 60°C. All dextran solutions were prepared at room temperature and equilibrated to the measuring temperature shortly before use.

Chemical characterization of the samples

Elemental analyses were performed in a varioMicro V1.4.1 system (Elementar Analysensysteme GmbH, Hanau, Germany) using the CHNS mode.

Moisture content of the samples was determined in a Moisture Analyser Sartorius MA 40 (Sartorius, Göttingen, Germany).

Equilibrium dialysis of the carrageenan solutions

An adequate amount of the sample was slowly added to the given volume of solvent (0.1*M* $NaNO_3$ with $\sim$ 20 mg NaN_3 per liter) to prepare stock solutions of $\sim$ 1.5 mg mL^{-1} by placing the dispersions in a water bath at 90°C for 10 min. Equilibrium dialysis at 25 and 60°C for all carrageenan solutions was performed against the solvent using Spectra/Por3 membranes (MWCO 3500) (Spectrum Europe, Breda, The Netherlands). Dialysis at 25°C was let to run over 24 h (slight stirring for accelerating the exchange), whereas at 60°C, dialysis was finished after 41 h (no stirring inside the oven). The exact polymer concentration after dialysis was calculated by taking into account the moisture content of the sample and the change of the solution volume (by weight) during dialysis.

Specific refractive index increment measurements

The refractive index increment $\partial n/\partial c$ between the dialysed solution and the dialysate of each

carrageenan was determined with a Brice-Phoenix differential refractometer, model BP-2000-V (Phoenix Precision Instruments, Philadelphia, PA). Measurements were done at 25°C (after equilibrium dialysis at 25°C) and 60°C (after equilibrium dialysis at 60°C), at four wavelengths, namely, 436, 546, 578, and 633 nm on concentration series (sets of five) prepared from the dialysed stock solution by dilution with the respective dialysate.

Dextran solutions (set of five each; without dialysis) were taken at 25 and 60°C. The refractometer was calibrated by means of NaCl at each used wavelength.

Light scattering standing alone—Batch mode measurements (MALS)

A DAWN HELEOS 109-HHC equipped with a F2 sample cell (Wyatt Technology) was used for all batch mode measurements. The wavelength of the incident light beam was $\lambda_0 = 659$ nm. Calibration was performed with toluene at 25°C. The instrument was rinsed with the pure solvent by means of a Shimadzu HPLC pump (0.5 mL min^{-1}) connected to a Rheodyne injector with a 2.0-mL loop inside a Shimadzu column oven keeping the temperature prior to injection at the specified measuring temperature.

Concentration series were prepared from stock solutions ($\sim$ 2 mg mL^{-1}) by dilution and injected through a 0.2-μm pore size membrane filter (Nylon Millex-GN filter units from Millipore, Billerica, MA) in the order of increasing concentration (two injections per concentration). The recorded peaks representing the Rayleigh ratio were manually defined. All polymer concentrations were related to the dry matter content. The data were plotted according to Zimm using the ASTRA V software.

HPSEC with on-line MALS and viscometry detection

The HPSEC system consisted of an Agilent 1100 HPLC system with degasser (Agilent Technologies, Santa Clara, CA), two serially connected SHOKO-WYATT SEC columns within a Shimadzu column oven, a Rheodyne manual injector, and PID-thermoregulated tubes to connect the individual parts of the equipment. The resultant void and total volume of the separation system was $\sim$ 19.2 and $\sim$ 39.5 mL, respectively. The flow speed of the eluant was adjusted to 0.6 mL min^{-1} and the injected (through 0.2 μm pore size membrane filters as earlier) sample volume was 200 μL. The light scattering monitor was either a DAWN EOS003 ($\lambda_0 = 658$ nm) or a DAWN HELEOS ($\lambda_0 = 659$ nm) equipped with a K5 sample cell and calibrated with toluene at 25°C. We used a differential refractometer Optilab rEX (Wyatt Technology) with an operating wavelength of 678 nm as a concentration monitor. The (precalibrated) Optilab rEX was used with a direct computer connection and needed no further calibration. A ViscoStar 112 (Wyatt Technology) was run with a dilution factor of 0.500. The whole procedure was run by the ASTRA V software, which was also used for all data manipulations. The 2nd virial coefficients were taken from the respective batch mode measurements. All angular dependences were plotted according to Zimm and fitted by a first-order fit.

RESULTS AND DISCUSSION

Chemical composition of the carrageenan samples

The elemental analyses yielded C : S ratios as high as 10.7 : 1 (kappa), 6.43 : 1 (iota), and 4.36 : 1 (lambda) instead of the ideal ratios such as 12 : 1, 6 : 1, and 4 : 1. Such deviations from the ideal formulae are consistent with $\sim$ 11% iota-segments in the applied kappa-carrageenan or 7% kappa-segments in the iota-carrageenan. Almost the same composition was found by H NMR[11,12] or NMR/IR[14] experiments on Sigma fine chemicals prior to and after purification.

The carbon content related to the dry matter was found to be 30.0% (kappa) and 28.0% (iota) and 22.4% (lambda).

Batch mode measurements

Calibration of the DAWN MALS instrument at 25 and 60°C

To convert the measured relative scattering ratios into absolute scattering intensities, the equipment has to be calibrated. This is normally done by means of toluene, the absolute scattering intensity of which at 25°C for specified wavelengths is known. By the temperature-dependent refractive index of the solvent, the scattering volume depends on temperature. Therefore, the calibration constant is supposed to depend on temperature as well,[23,24] and the instrument calibration should be performed at each measuring temperature. Unfortunately, absolute scattering intensities of toluene or other pure solvents at elevated temperatures are not available, so the use of toluene at 60°C would fail. Instead, one can apply lattices or any sufficiently small polymer of exactly known molar mass which is known not to undergo temperature-dependent changes. The latter is what we did. Using a calibration standard dextran of $M_w = 4 \times 10^4$ g mol^{-1}, we carried out measurements at 25 and 60°C using the same set of polymer solutions. A representative Zimm plot is given in Figure 1. It shows the anticipated grid of parallel straight lines for the concentration and angular

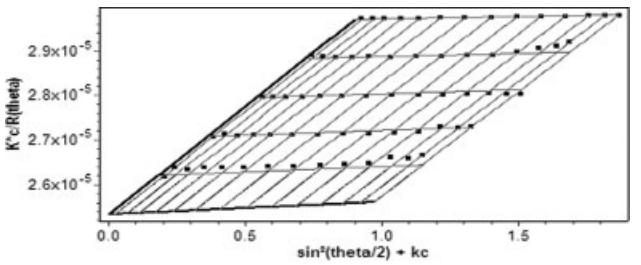

Figure 1 Zimm plot of the calibration standard dextran having an average molar mass. $M_w = 4 \times 10^4$ g mol^{-1}; solvent: 0.1*M* $NaNO_3$, $T = 25$°C.

dependence where the angle of observation ranges from 18° to 160°. Making use of the same calibration constant (based on toluene at 25°C), we obtained practically identical average molar masses (Table I); therefore, the theoretically predicted temperature effect on the calibration constant was small enough to be neglected in the following.

To calculate the molar masses in Table I, we took the bold-printed specific refractive index increments $\partial n/\partial c$ from Table II for $\lambda_0 = 659$ nm, which is the DAWN MALS operating wavelength. They were obtained by linear extrapolation of the other values measured at four shorter wavelengths.

In the case of dextran, the values vary only slightly with the temperature but decrease clearly with increasing wavelength. They meet reasonably well with those reported elsewhere,[25,26] which may well underpin the correctness of our measurements.

The $\partial n/\partial c$-values for dextran at 50 and 60°C may also be obtained by combining the mixture rule for binary solutions and the equations of Lorenz-Lorentz[24] and Eykman.[27] The values of the specific volume and the refractive index were taken from the literature.[28,29] Table II shows the calculated values to be nearly identical with the extrapolated ones.

Measurements on carrageenans at 25 and 60°C

Table II also compiles the $\partial n/\partial c$ values for the three types of carrageenans as they have been used throughout this contribution. Unlike Vreeman et al.,[1] we obtained almost ideal linear plots for Δn versus c in almost every experiment with n, the refractive index, and c, the polymer concentration, when we followed the common practice as described earlier. Compared with the relatively slight wavelength dependence, there is a strong temperature effect on $\partial n/\partial c$. All values at 60°C were found to be significantly higher than those at 25°C in good agreement with findings from elsewhere.[4] Altogether, the values in Table II differ from those given in the literature as the collection in Table III may illustrate. Our findings at 60°C indicate a systematic decrease of $\partial n/\partial c$ by about 15% with growing sulfate content comparable with Ref. 7. Only smaller differences and not even the same tendency were observed at 25°C.

Confronted with the issue of our experimental error, we would focus on the reliability of the concentration data after dialysis and estimate the error not to exceed ±5%. This may seem relatively high but a critical survey of the polysaccharide literature would seldom yield much better precision. At least in parts, difficulties of concentration determination may well account for the variety of the reported $\partial n/\partial c$ values of carrageenans. An error of ±5% in $\partial n/\partial c$ means a systematic error of ±10% in the molar mass M_w because of the quadratic term in the optical constant (Refs. 23 and 26, or any textbook).

Figure 2 presents a collection of Zimm plots obtained on kappa-carrageenan. To test possible influences of the dissolution and/or measuring temperature on the solution behavior, the sample was dissolved and analyzed at 25°C or, alternatively, dissolved at 90°C and measured at 25 and 60°C, respectively. Aliquot parts from the same concentration series were taken throughout this experiment. Thus, other than the desired, preparative effects should be prevented. Dissolution and measuring at 25°C led to a characteristically distorted Zimm plot. The distortion comes from the increasing downward curvature with rising concentration, and therefore fitting the angular dependence required a quadratic fit. At the same time, the concentration dependence could be fitted reasonably well by a first-order fit.

A rather similarly shaped but somewhat less distorted Zimm plot was obtained when the sample

TABLE I
Test of the MALS Equipment at 25 and 60°C Using a Commercial Dextran ($M_w = 4 \times 10^4$ g mol^{-1}) Calibration Standard

T (°C)	$\partial n/\partial c$ (mL g^{-1})	M_w (g mol^{-1})	$B \times 10^4$ (mL mol g^{-2})	R_z (nm)
25	0.149	39480 ± 50	4.868 ± 0.045	7.2 ± 0.9
60	0.147	39670 ± 80	4.213 ± 0.065	5.6 ± 1.7

Calibration constant $K_{MALS} = 2.3396 \times 10^{-4}$ based on toluene at 25°C.

TABLE II
Specific Refractive Index Increments $\partial n/\partial c$ in mL g^{-1} as Function of Wavelength and Temperature in 0.1*M* $NaNO_3$ (all Polymer Concentrations Related to Dry Matter)

Sample	*T* (°C)	436 nm	546 nm	578 nm	633 nm	659 nm Extrapolated	659 nm Calculated
Dextran	25	0.1549	0.1523	0.1517	0.1496	0.149	
Dextran	50	0.1535	0.1510	0.1503	0.1484	0.149	0.148
Dextran	60	0.1530	0.1504	0.1505	0.1491	0.147	0.148
κ-carr	25	0.1110	0.1089	0.1092	0.1068	0.107	
κ-carr	60	0.1319	0.1300	0.1295	0.1261	0.127	
ι-carr	25	0.0948	0.0944	0.0952	0.0925	0.093	
ι-carr	60	0.1202	0.1211	0.1232	0.1183	0.120	
λ-carr	25	0.0983	0.0967	0.0990	0.0974	0.097	
λ-carr	60	0.1128	0.1089	0.1103	0.1077	0.107	

had been heated up to 90°C and was then analyzed at 25°C. In this case, the concentration-dependent curvature of the angular dependence is still there but distinctly reduced. Again, the concentration dependence at each angle of observation could be described by straight lines (first-order fit).

Finally, the Zimm plot obtained at 60°C reveals an almost "ideal" shape (similar to dextran in Fig. 1). Accepting the visible deviations of up to 5% between several measuring points and the respective extrapolated ones, both the angular dependence (between 25° and 160°) and concentration

TABLE III
Selected Specific Refractive Index Increments of Carrageenans as Given in the Quoted Literature

Sample	Solvent	*T* (°C)	Wavelength (nm)	$\partial n/\partial c$ (mL g^{-1})	Ref.	Comments
κ-carr Na^+	0.1*M* NaCl plus 0.005 M EDTA, pH 6.7	20	546	0.118 ± 0.003	1	Equilibrium dialysis (solvent/solution) for each member of the concentration series (quite unusual procedure).
κ-carr Na^+	0.1*M* NaCl		633	0.149	3	Temperature not explicitly given, probably 25°C.
	0.05*M* NaCl			0.145		
	0.1*M* NaI			0.150		
	0.05*M* NaI			0.150		
ι-carr Na^+	0.1*M* NaCl	25		0.124 ± 0.020	4	Wavelength not explicitly given, probably 546 nm.
		69		0.147 ± 0.018		
ι-carr K^+	0.1*M* KCl	25		0.124 ± 0.020		
		69		0.147 ± 0.018		
κ-carr	0.1*M* NaCl	Variable	436	Variable	5	Data inconsistent (Figs.3 and 4) but distinct *T* effects.
λ-carr	0.1*M* NaCl			0.116 ± 0.002	6	Temperature not explicitly given, probably 25°C; wavelength not explicitly given, probably 633 or 515 nm.
κ-carr Na^+	0.1*M* NaCl	25	633	0.149 ± 0.005	7	$\partial n/\partial c$ determined in aqueous NaCl, but HPSEC in 0.1 M $NaNO_3$ as eluant
	0.05*M* NaCl			0.145 ± 0.005		
λ-carr Na^+	0.1*M* NaCl	25	633	0.108 ± 0.013		
	0.05*M* NaCl			0.116 ± 0.002		
κ-carr	0.1*M* LiI	25	633	0.136	12	Independent observation: cooling from 70 to 25°C caused an increased by 10% peak area of the HPSEC elution line (DRI detector); attributed to order/disorder transition only
κ-carr	0.01*M* LiCl		633	0.122		
ι-carr	0.2*M* LiCl		633	0.105		
ι-carr	0.01*M* LiCl		633	0.105		
κ-carr	0.1*M* NaCl	25		0.148	13	
ι-carr				0.127		

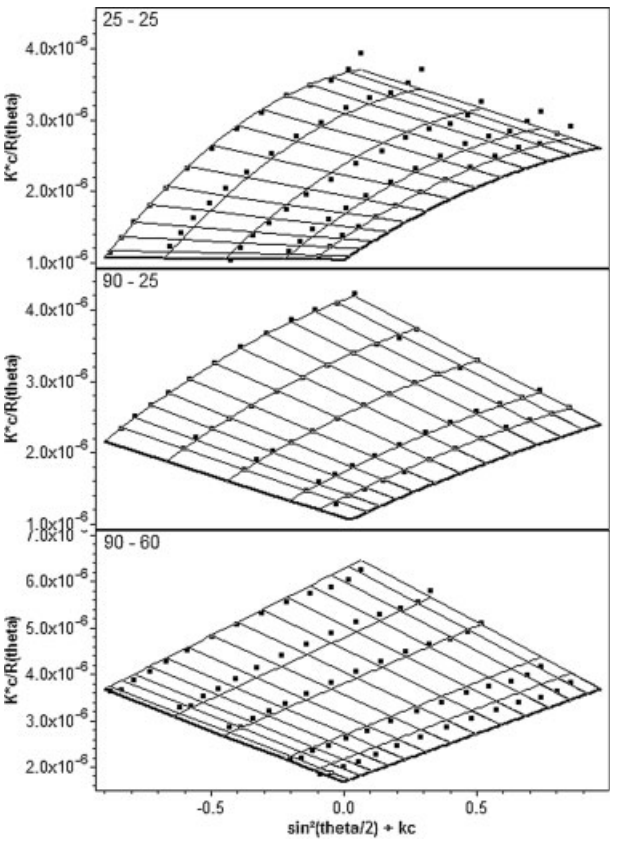

Figure 2 Series of Zimm plots obtained on κ-carrageenan in 0.1*M* $NaNO_3$ (arbitrary constant $k = -898.5$). Top: dissolution (overnight) and measurement at 25°C. Middle: dissolution at 90°C (≈10 min) and measurement at 25°C. Bottom: dissolution at 90°C (≈10 min) and measurement at 60°C.

dependence could be fitted best by straight lines. (Regarding the angular dependence, this decision gets support from HPSEC/on-line MALS, see Fig. 6.) This is what we expect to find in the case of molecularly disperse solutions of (relatively) flexible chains having a moderately broad molar mass distribution (e.g., polydispersities of $M_w/M_n \approx 2$ with M_w, the weight average molar mass, and M_n, the number-average molar mass). It seems fair to mention that the small arbitrary constants in all our Zimm plots allow detailed insights into the quality of the measurements, whereas the elsewhere used big arbitrary constants[1–3,17] make the angular dependence extremely steep thus giving the resultant Zimm plots a deceptive beauty and hiding the concentration-dependent angular dependence. Other papers among the quoted ones present only the extrapolated concentration dependence at zero angle[14] or the angular dependence at zero or another single concentration[15]; therefore, one cannot see any details and develop a mind of one's own.

Table IV contains the respective molecular parameters as derived by the ASTRA software along with the experimental error each (without possible systematic errors). The weight-average molar mass of kappa-carrageenan was found to be $M_w \approx 5.96 \times 10^5$ g mol^{-1} at 60°C, whereas both measurements at 25°C indicate an increased by roughly 60% M_w. The increase of M_w is accompanied by an increase of the *z*-average root mean square radius of gyration R_z from 74 to 87 and 104 nm, respectively. Parallel with the increase of M_w, the second virial coefficient B decreases from $\sim 1 \times 10^{-3}$ to 1×10^{-4} mL mol g^{-2} for the never heated solution via $\sim 5 \times 10^{-4}$ mL mol g^{-2} for the previously heated solution.

In the given context, we would interpret these findings as follows:

- A molecularly dispersed solution was present at 60°C. This is concluded from the shape of the Zimm plot along with the B value. The latter is in reasonably good agreement with what the excluded volume theory predicts for a coil-like polyelectrolyte in a thermodynamically good solvent if charge effects are suppressed by added salt. (Whether previous heating up to 90°C was effectual or not remains open.)
- In the previously heated and then cooled to 25°C solution, some species of the initially molecularly dispersed population associate. The extent of association grows with rising polymer concentration. This is suggested by (i) the concentration-dependent curvature of the angular dependence indicating a steadily growing polydispersity of the population, (ii) the correspondingly lowered B value as expression for the concentration-dependent apparent average molar mass $M_{w,app}$, and (iii) the increased M_w at zero concentration.
- The solubility of the polymer at room temperature depends on the concentration. Obviously, a molecularly dispersed solution could not be prepared at all. The proportion of incompletely dissolved associates grows with increasing polymer concentration. This is derived from the increasing downward curvature of the angular dependence leading to an even lower B compared with the preheated solution at 25°C along with the increased M_w when compared with that at 60°C.

Although our experiments revealed aggregates at 25°C, Vreeman et al.[1] obtained undistorted Zimm plots at similar conditions (room temperature and ionic strengths near 0.1*M* sodium by added sodium chloride, see later). Presumably, the presence of 11% iota-segments in our sample and/or minor amounts of potassium ions is sufficient to induce aggregation.

TABLE IV
Results of Batch Mode MALS Measurements on Carrageenans at 25 and 60°C

Sample	Temperature (°C) for dissolution	Measuring temperature T (°C)	$\partial n/\partial c$ (mL g^{-1})	$M_w \times 10^{-5}$ (g mol^{-1})	$B \times 10^4$ (mL mol g^{-2})	R_z (nm)
kappa	90 (10 min)	60	0.127	5.963 ± 0.231	9.917 ± 0.446	74.3 ± 3.4
	90 (10 min)	25	0.107	9.406 ± 0.283	5.470 ± 0.217	86.8 ± 3.8
			(0.127)	(6.677 ± 0.201)	(7.706 ± 0.305)	(86.8 ± 3.8)
	25 (overnight)	25	0.107	9.595 ± 0.522	0.125 ± 0.340	104.3 ± 9.8
			(0.127)	(6.811 ± 0.370)	(0.177 ± 0.478)	(104.3 ± 9.8)
iota	90 (10 min)	60	0.120	8.336 ± 0.349	2.243 ± 0.037	86.3 ± 3.6
	90 (10 min)	25	0.093	292.3 ± 19.1	0.003 ± 0.001	307.1 ± 9.9
	25 (overnight)	25	n.d.	n.d.	n.d.	n.d.
lambda	90 (10 min)	60	0.107	14.01 ± 1.08	10.15 ± 0.043	93.1 ± 6.4
	90 (10 min)	25	0.097	14.85 ± 0.39	6.214 ± 0.124	110.6 ± 3.8
	25 (overnight)	25	0.097	13.18 ± 0.43	4.845 ± 0.171	101.6 ± 5.6

n.d., not determined.

In summary, our results confirm the need of elevated temperature to reach full polymer solubility in the case of industrial samples.

In the literature, undistorted Zimm plots of kappa-carrageenan at room temperature are an exception rather than the rule. Some authors[4] omitted all measuring points below the angle of observation of 50° arguing with aggregates as impurities dominating the low-angle domain. Others[6] extrapolated solely the measuring points for angles between 25 and 90° arguing with the postulated stiffness of chains. Semenova et al.[5] ascribed the curvature to a two-component system choosing an oversimplifying interpretation. Thus, all derived parameters are highly questionable as systematic studies on two-component[30] or aggregating systems[31] or stiff chains[32] may illustrate.

Similar to our light scattering data at 25°C, sedimentation equilibrium experiments in the analytical ultracentrifuge on kappa-carrageenan[33] yielded a B value near zero. Trying to give an explanation, the authors denied the possibility of association between like-charged species. This point of view cannot be accepted. It fully ignores the screening by counter ions at an ionic strength of 0.1M. Screening effects are the essence of the theory of polyelectrolyte behaviour in aqueous solution.

To illustrate the huge effect of the specific refractive index increment, we have made calculations assuming a temperature-independent value $\partial n/\partial c = 0.127$ mL g^{-1} (Table IV). This would change the situation completely. M_w at 25 and 60°C would then be almost the same. B would depend on the procedure as described earlier, whereas the radius R_z remains unchanged for the unchanged angular dependence. Consequently, one would not only deny any remarkable association but, by comparison of the first and the third line, erroneously conclude on a more extended "stiffer" conformation at 25°C in the never heated solution (helix vs. coil discussion). This will say that sometimes the correct radius of gyration is easier to obtain than the correct respective molar mass. Thus, wrong $\partial n/\partial c$ values might be the major source of the confusion in the quoted literature. Attempts to conclude from a scattering intensity on the specific refractive index increment[15] must be rejected anyway, see e.g., Ref. 23.

Figures 3 and 4 along with Table IV show the corresponding results for iota- and lambda-carrageenan. Iota-crrageenan did not properly dissolve at room temperature, so the measurements had to be confined to 25 and 60°C after heating up to 90°C.

These two carrageenans follow the same pattern as discussed for kappa-carrageenan. It turns out that 60°C in 0.1M $NaNO_3$ is a good condition for the macromolecular characterization of all three types of carrageenans without a marked interference by aggregates.

Despite lots in common, a few differences do exist when we consider the details.

- In the order of increasing sulfate content, the average molar masses increase from 5.96×10^5 via 8.34×10^5 to 1.4×10^6 g mol^{-1}. All B values at 60°C are close to 1×10^{-3} mL mol g^{-2}.
- The immense increase of M_w for iota-carrageenan at 25°C has no equivalent in the case of lambda-carrageenan, the molar mass of which remains the same under all conditions. However, the same molar masses result from differently shaped Zimm plots. Consequently, lambda-carrageenan is the only member of the family for which temperature effects on M_w become minimized at infinite dilution compared with the findings at various salt concentrations in Ref. 8.

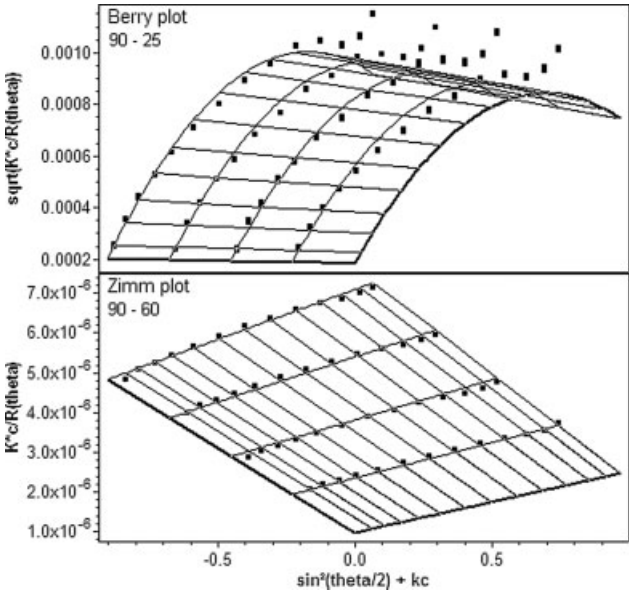

Figure 3 Series of plots obtained on ι-carrageenan in 0.1*M* $NaNO_3$. Top: dissolution at 90°C (≈10 min) and measurement at 25°C. Bottom: dissolution at 90°C (≈10 min) and measurement at 60°C.

HPSEC coupled with on-line MALS plus viscometry and concentration (DRI) detection

Calibration and testing the system—Methodological aspects

Batch mode measurements have suggested 60°C to be a good choice for HPSEC when the studies are aimed at the characterization of nonaggregated molecules. Complementary HPSEC runs at 25°C might then help to learn more about possibly aggregated (but still soluble) material.

Before starting the carrageen analyses, we checked the instruments' performance in the given configuration. Therefore, known amounts of two dextran calibration standards were injected while the equipment was run at either 25 or 60°C. The high-molar mass dextran had an average molar mass $M_w \approx 5 \times 10^6$ g mol^{-1}, whereas the low-molar mass dextran with $M_w = 4 \times 10^4$ g mol^{-1} was the same as described in Figure 1 and Table I. Results of triple-detector HPSEC are shown in Figure 5 and Table V.

There is virtually no temperature effect on the elution behavior of the low-molar mass dextran. Peak position, molar mass calibration curve *M* versus elution time, and also the course of intrinsic viscosity [η] versus elution time coincide rather well. In the case of the high-molar mass dextran, heating up the system leads to a somewhat faster polymer elution and somewhat lower intrinsic viscosities.

Table V shows ~ 10% higher recovery rates at 60°C (although ~ 3% volume expansion of the warm sample solution was neglected), whereas the respective average molar masses appear decreased by almost the same percentage. The value found for the low-molar mass dextran at 25°C agrees perfectly with that from Table I. The percentage in brackets below $[\eta]_w$, M_w, and also M_w/M_n was provided by the ASTRA V software. It describes solely the statistical uncertainty of the measurement but does not include any of the many possible systematic errors. Therefore, it is no measure of the correctness of data. Tables V–VII altogether made us think that the concentration determination was the most delicate point of the procedure with secondary effects on *M* and [η]. The deviations of M_w and $[\eta]_w$ are therefore assumed to reflect the total experimental error inherent in the method covering both statistical and systematic errors. In our experience, reproduction of (correct) average molar masses within 10% is not that bad in the polysaccharide domain.

The index "*w*" on *M* and [η] in Table V and all the following ones as well as the polydispersity M_w/M_n require a critical evaluation of what multidetector HPSEC can provide. The ASTRA software (and

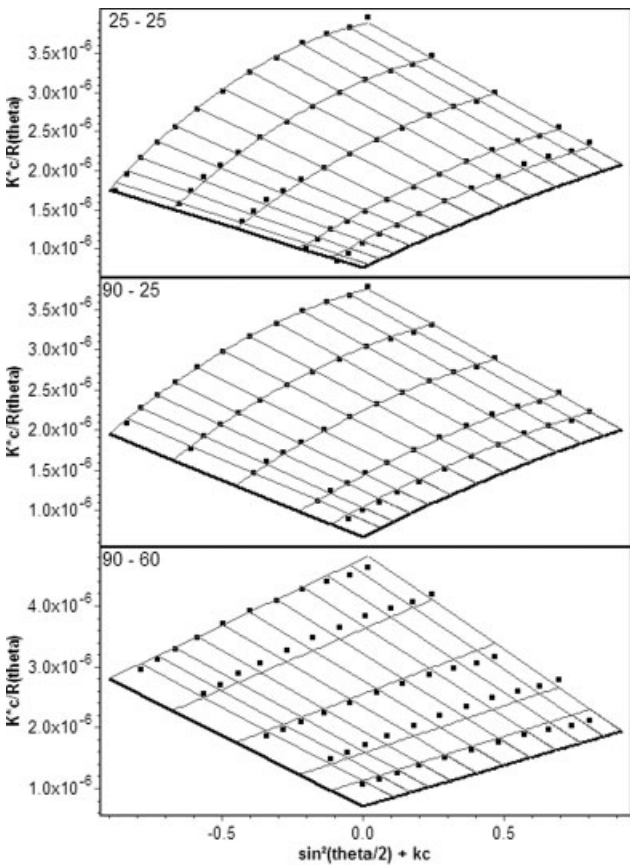

Figure 4 Series of Zimm plots obtained on λ-carrageenan in 0.1*M* $NaNO_3$. Top: dissolution (overnight) and measurement at 25°C. Middle: dissolution at 90°C (≈10 min) and measurement at 25°C. Bottom: dissolution at 90°C (≈10 min) and measurement at 60°C.

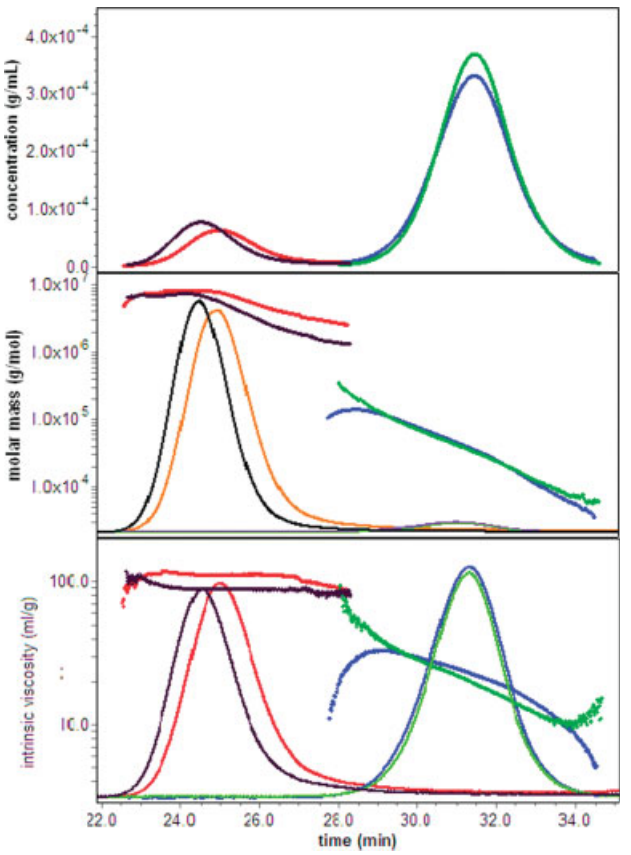

Figure 5 HPSEC on dextrans at 25 and 60°C—testing the analyzing system. Pink circles: 5×10^6 g mol^{-1} and 25°C; blue circles: 4×10^4 g mol^{-1} and 25°C. Black circles: 5×10^6 g mol^{-1} and 60°C; green circles: 4×10^4 g mol^{-1} and 60°C. Top: concentration versus elution time. Middle: molar mass and Rayleigh's ratio versus elution time. Bottom: intrinsic and specific viscosities versus elution time. [Color figure can be viewed in the online issue, which is available at www.interscience.wiley.com.]

other firms' products as well) assumes all slices to be monodisperse with respect to molar mass ($M_n = M_w = M_z \equiv M$ without index) and calculates the different moments of M in terms of M_n, M_w, and M_z. The same applies to the root-mean-square radius of gyration R and the intrinsic viscosity [η]). In reality, the condition of monodisperse slices cannot be reached. M and R by light scattering remain, in fact, M_w and R_z even when measured on HPSEC slices. Taking notice of these facts complicates, the situation considerably but, making comprehensive use of the data herein, we have to deal with the consequences on (*x*) the two derivable Mark-Houwink type plots and (*xi*) all kinds of average parameters meant to characterize the sample as a whole.

First, the ASTRA "conformation plot" denotes a double-logarithmic plot of the root-mean-square radius of gyration versus molar mass. Correctly, one would have to add the indices "*z*" and "*w*," respectively. The scaling exponent (slope) is said to allow conclusions on the conformation of the solute. However, in the framework of the generally accepted theory, this is linked with the condition of either monodispersity or at least constant polydispersity within a sample series. None of the two is realized in chromatographic practice.[20,32] Polydispersity is known to increase in the course of elution (peak broadening), so the different moments of the two parameters make the line flatter than it should be ideally. Therefore, any experimentally found scaling exponent reflects not only the macromolecules conformation but also the quality of separation. This may explain the occasionally presented strong and abrupt changes of the scaling exponent for different molar mass regions of polymer homologous linear chains[34,35] or values far below the theoretical limit for the given polymer.[36] Calculations that are based upon the scaling exponent[19] may then lead to false wormlike chain (WLC) parameters.

The situation with the [η]-*M* plot is similar. However, the high scaling exponents as typically found for linear polysaccharides inclusive carrageenans[1] (owing to excluded volume and/or draining effects rather than chain stiffness) minimize the addressed problem[37] and polydispersity effects may be neglected. Nevertheless, the quantitative interpretation in terms of WLC parameters is known to be problematical, see e.g., Ref. 21.

Secondy, let us consider M_w/M_n. $M_w = \sum_i (c_i M_i)/\sum_i c_i$ is supposed to come out correctly. Both c_i and M_i—the concentration and the respective molar mass in the *i*th slice—are measured directly, so the calculation needs no assumptions. The situation with M_n defined by $M_n = \sum_i n_i M_i /$

TABLE V
Results from Multiple-Detector HPSEC on Dextrans ($\partial n/\partial c$ from Table II and *B* from Table I)

Sample g mol^{-1}	Temperature (°C)	$\partial n/\partial c$ (mL g^{-1})	$B \times 10^4$ (mL mol g^{-2})	Recovery rate (%)	$[\eta]_w$ (mL g^{-1})	M_w (g mol^{-1})	$a_{[\eta]}$[a]	M_w/M_n
Dextran $\approx 5 \times 10^6$	25	0.149	1.834[b]	83	109.0 (0.1%)	6.302×10^6 (0.9%)	~ 0	1.093 (1%)
Dextran $\approx 5 \times 10^6$	60	0.147	1.834[b]	94	87.9 (0.3%)	5.460×10^6 (0.4%)	~ 0	1.189 (0.8%)
Dextran 4×10^4	25	0.149	4.868	93	21.9 (0.1%)	39,430 (2%)	(0.38)	1.501 (10%)
Dextran 4×10^4	60	0.147	4.213	101	19.4 (2%)	36,050 (2%)	0.52	1.364 (8%)

[a] Scaling exponent of the [η]-*M* relationship.
[b] Taken from measurements not shown here.

TABLE VI
Multiple-Detector HPSEC—Loading Effects on Results: kappa-Carrageenan (T = 60°C; $\partial n/\partial c$ = 0.127 mL g^{-1})

Injected amount (mg)	$B \times 10^4$ (mL mol g^{-2})	Recovery rate (%)	$[\eta]_w$ (mL g^{-1})	$M_w \times 10^5$ (g mol^{-1})	R_w (nm)	M_w/M_n
0.3	9.917	83	895.5	3.831	72.1	1.733
0.6	9.917	86	801.6	3.408	69.8	1.395
0.6	9.917	89	812.7	3.327	69.0	1.453
0.6	0	89	812.7	3.109	66.7	1.427

$\sum_i n_i = \sum_i c_i / \sum_i c_i/M_i$ is different. n_i cannot be measured directly but is obtained from $n_i = c_i/M_i$, which is valid for a monodisperse system only. For any polydisperse system, M_n would be an overestimate thus producing an underestimate of M_w/M_n. This will say that solely an ideal separation would give a correct polydispersity. The poorer the separation, the smaller is the apparent value reaching 1.0 for no separation at all. Thus, knowing the correct polydispersity of the sample under study, one can benefit from such calculations so as to judge the quality of separation. Reasonable values close to 2 or above can be found in the carrageenan literature[7,14] besides highly suspicious ones as low as 1.1.[10] Preparation of such narrowly distributed samples would be extremely difficult if not impossible.

Finally, the calculated number-average value M_n for the sample as a whole is different from what would be found by end-group determination or osmometry,– see Refs. 1 and 6. Precisely, it has the meaning of $(M_w)_n$ while the calculated weight-average radius of gyration has the meaning of $(R_z)_w$. After due consideration, we believe that only a few average parameters out of the software-provided set are useful, namely M_w, $(R_z)_w \equiv R_w$, $[\eta]_w$ and M_w/M_n. Therefore, all tables contain only these ones completed by the respective scaling exponents a_R and $a_{[\eta]}$.

Now we return to Figure 5 and Table V. Like the majority of polysaccharides inclusive carrageenans,[1] the applied dextrans are supposed to have a polydispersity $M_w/M_n \approx 2$. If so, the actually found values in Table V along with the unreasonably low scaling exponents $a_{[\eta]}$ are hints on almost no separation of dextran with $M_w \approx 5 \times 10^6$ g mol^{-1} and a distinctly better separation of dextran with $M_w = 4 \times 10^4$ g mol^{-1}. (The correctness of this interpretation could be easily checked by using another separation medium.) This, however, is of no consequences for the following carrageenan analyses.

Searching for good separation conditions for carrageenans

Good separation conditions must be discovered by experiment. Particularly, loading effects are known to play a big part. On the one hand, the injected polymer amount must be high enough to ensure a reasonable signal-to-noise ratio on all three detectors. On the other hand, overloading the columns is known to deteriorate separation. Therefore, we studied possible effects of the injected polymer amount first.

Figure 6 displays our findings when the concentration of the injected solution was 3 and 1.5 mg mL^{-1}, respectively. A collection of measured angular dependences is included to show the quality of the light scattering part when compared with Figure 2. The excellent reproducibility is demonstrated by the nearly identical course of the green and blue lines. However, reduction to half the amount leads to a distinctly narrower concentration peak. The respective broader (cumulative) molar mass distribution curve (inset), the steeper line in the conformation plot (a_R increases from $\sim$ 0.55 to 0.61), and the straightened $[\eta]$-M curve (all in red) are all indicative of a remarkably improved separation because

TABLE VII
Results from Multiple-Detector HPSEC ($\partial n/\partial c$ from Table II and B from Table IV)

Sample	$\partial n/\partial c$ (mL g^{-1})	B (mL mol g^{-2})	Recovery rate (%)	$[\eta]_w$ (mL g^{-1})	$M_w \times 10^{-4}$ (g mol^{-1})	R_w (nm)	a_R[a]	$a_{[\eta]}$[b]	M_w/M_n
Degraded κ-carr	0.127	9.917×10^{-4}	n.d.	61.9 (0.1%)	2.393 (8%)	16.6 (133%)	n.d.	0.96	1.568 (19%)
κ-carr	0.127	9.917×10^{-4}	88	778.3 (0.1%)	44.61 (3%)	69.9 (5%)	0.68	0.83	1.902 (13%)
ι-carr	0.120	2.243×10^{-3}	99	693.7 (0.1%)	47.31 (3%)	70.9 (5%)	0.68	0.77	2.028 (14%)
λ-carr	0.107	1.015×10^{-3}	106	1212.9 (0.1%)	92.17 (5%)	109.3 (2%)	0.64	0.83	1.540 (7%)

n.d., not determined.
[a] Scaling exponent of the "conformation plot," which means root mean square radius of gyration versus molar mass.
[b] Scaling exponent of the $[\eta]$-M relationship.

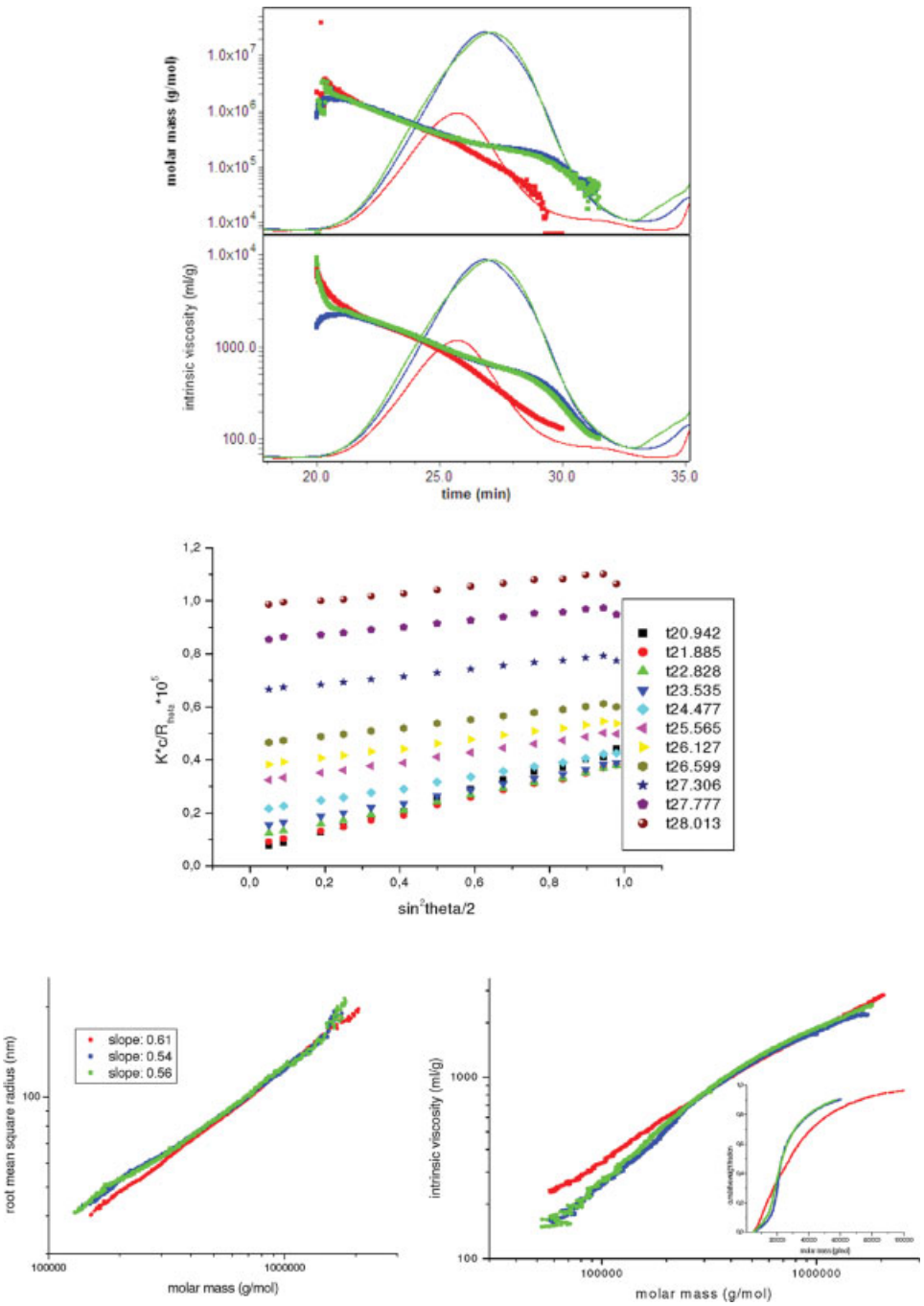

Figure 6 Effect of loading concentration on HPSEC separation; kappa-carrageenan at 60°C; red circles: 1.5 mg mL^{-1}; blue and green circles: 3 mg mL^{-1}. Top: molar mass and refractive index trace versus elution time. Upper middle: intrinsic viscosity and refractive index trace versus elution time. Lower middle: collection of measured angular dependences on "HPSEC slices." Bottom left: "conformation plot"; bottom right: [η]-M_w plot with MWD (inset). [Color figure can be viewed in the online issue, which is available at www.interscience.wiley.com.]

high-molar mass fractions are no longer spread over the low-molar mass range. Consistently, M_w/M_n in Table VI moves from 1.4 to 1.7 but remains distinctly below 2.0 in this experiment (see Table VII). Practically, identical recovery rates as well as M_w and $[\eta]_w$ are obtained. (None of the three is supposed to depend on the quality of separation.) Note: Taking B into account or not (Table VI lowest line) makes a difference of 4% in M_w despite the low polymer concentration in the eluant.

In favor of a good signal-to-noise ratio, we did not test even smaller loading concentrations but injected about 0.3 mg for all subsequent SEC runs (if not given otherwise).

Loading effects as shown in Figure 6 illustrate the earlier discussion very well. Ignoring such effects

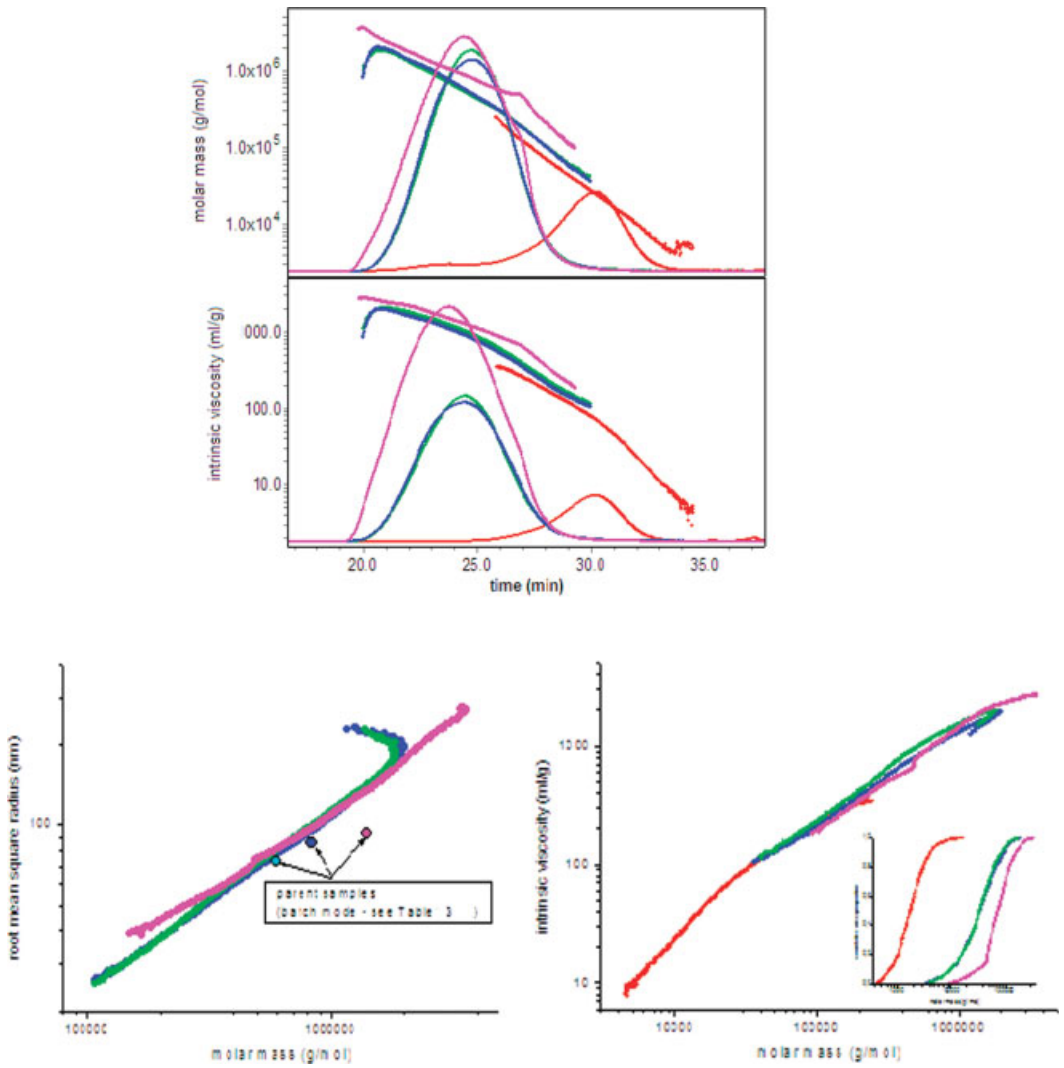

Figure 7 HPSEC on carrageenans; loading concentration: 1.5 mg mL^{-1}. Pink circles: λ-carr.; blue circles: ι-carr.; green circles: κ-carr.; red circles: degraded κ-carr. Top: molar mass and Rayleigh's ratio versus elution time. Middle: intrinsic and specific viscosity versus elution time. Bottom left: "conformation plot"; bottom right: [η]-M_w plot with MWD (inset). [Color figure can be viewed in the online issue, which is available at www.interscience.wiley.com.]

has led to absurd conclusions. Some authors[38] proposed an on-line determination of 2nd virial coefficients as a function of the molar mass from a series of SEC runs with various loading concentrations. The authors obtained steadily decreasing B values down to even negative ones in the order of decreasing molar masses. This is not only in conflict with the theory[37,39] and elsewhere measured values[1] but also with common sense for the particularly good solubility of low molar mass fractions.

Comparative studies on carrageenans

Figure 7 collects our results on the three types of carrageenans. In addition, a degraded kappa-carrageenan was analyzed (roughly fivefold polymer amount injected). Compared with the data published by the Marinalg International Group,[40] we could achieve a much better separation across the whole molar mass range from $\sim 5 \times 10^3$ to 3×10^6 g mol^{-1}. This is suggested equally well by MALS and viscosity detection. The respective figures are collected in Table VII. The statistical uncertainty of the measurements is satisfactorily low for the most derived parameters but [η] or $[\eta]_w$ can be measured best. This is worth to be kept in mind in view of routine analyses since no risky operation such as the MALS calibration is needed.

$M_w/M_n \approx 2$ for kappa- and iota-carrageenan signals a very fine separation and gives the respective scaling exponents of $a_R = 0.68$ and $a_{[\eta]} \approx 0.8$ a high extent of reliability. Correspondingly, there is indication of a somewhat poorer separation of the degraded kappa-carrageenan and the high-molar mass lambda-carrageenan. This is consistent with our general understanding of SEC according to

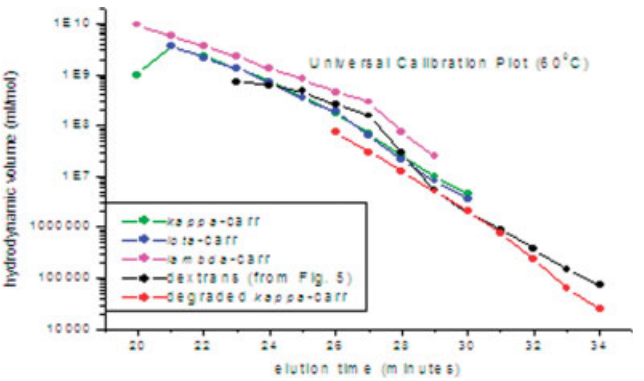

Figure 8 Universal Calibration Plot (hydrodynamic volume $\{M_w \cdot [\eta]\}$ versus elution time) (M_w and $[\eta]$ taken from Figs. 5 and 7). [Color figure can be viewed in the online issue, which is available at www.interscience.wiley.com.]

which the efficiency of the columns goes down near the edges of the separation range.

Compared with the data in Table IV, all M_w values appear significantly decreased. Factors vary from 0.57 (iota) to 0.75 (kappa) via 0.7 (lambda), whereas Slootmaekers et al.[7] reported on nearly identical average molar masses of kappa- and lambda-carrageenan from different techniques (low-angle-laser light scattering, "classical" light scattering, sedimentation-diffusion analyses with the diffusion coefficient from dynamic light scattering). We have no conclusive explanation but tend to deny the possibility of high-molar mass components adsorption on the columns. Maybe the software overcorrects some data, for example, when at the beginning polymer elution, the concentration is extremely low but M is high and much depends on the baseline settings (apart from strongly scattering data anyway). In this area, the error of M can easily reach 100%. Moreover, the software supplier does not describe whether the calculation is based upon a "smoothened" and linearly extrapolated calibration curve (log M versus elution time) or follows directly the presented graph inclusive the certainly wrong downward curvature at the beginning. The ASTRA Help just mentions that unreasonable (negative or strongly insecure) values are automatically omitted. Consequently, each value must be considered with care and seen in the whole context. As we used to do on other polysaccharides,[20,21] we would give the batch mode data preference as soon as the sample is addressed as a whole, e.g., in comparison with osmometry or sedimentation analysis in the analytical ultracentrifuge. Some curious examples[41] have already illustrated the limits of multi-detector-HPSEC.

Despite the described discrepancies, the points for two of the three parent samples (Table IV) match the HPSEC data in the conformation plot fairly well.

Particularly, the $[\eta]$-M plot in Figure 7 deserves attention. Unlike findings from elsewhere,[42] all samples form a slightly curved joint $[\eta]$-M line covering a molar mass range from $\sim 5 \times 10^3$ to 3×10^6 g mol^{-1}. This is, indeed, what we had expected to find in view of the strong structural relationship of all three carrageenan types. The curvature becomes understandable on the background of the WLC model.[43]

A universal calibration plot[44] is shown in Figure 8. Although the curves regionally overlap reasonably well we would not take that plot for an appropriate substitute of direct molar mass detection. This is not the place to make a statement on the validity of the principle of universal calibration, but in our own studies universal calibration has always been superior to the proposal made in Ref. 45.

In this paragraph, we have presented conclusive evidence for the strong similarity of the macromolecular characteristics and solution behavior of all three types of carrageenans at least in the disordered state at 60°C in 0.1M $NaNO_3$ as solvent. The use of strictly "clean" polymer homologous series by the definition at the beginning in place of our somewhat "contaminated by each other" industrial samples would not make a difference.

Comparison of kappa-carrageenan by HPSEC at 25 and 60°C

Next, we compare HPSEC data on kappa-carrageenan, which were obtained at 60 and 25°C. A similar approach[12] using kappa- and iota-carrageenan in 0.2M LiCl or LiI suggested a temperature-induced doubling of the molar mass upon temperature decline, which was seen to indicate the formation of double-stranded chains in the ordered state. Figure 9 shows the originally obtained experimental data followed by the derived differential molar mass distribution, the $[\eta]$-M plot as well as the conformation plot. At a glance, the somewhat differing elution lines as well as the dissimilar course of M and $[\eta]$ versus elution time might well be due to temperature effects on both the separation medium (swelling) and the macromolecules size. The respective (differential) molar mass distribution curves, however, reveal a remarkable increase of high-molar mass fractions at 25°C at the cost of lower molar mass fractions. The peak maximum at $M \approx 3.5 \times 10^5$ g mol^{-1} remains nearly unchanged. It is hard to say whether the new-formed second maximum at $M \approx 8.8 \times 10^5$ g mol^{-1} fairly reflects the mass distribution of the high-molar mass species. Accumulation or, in other words, a rather poor separation in a special region may account for the apparently slight increase of M_w/M_n from $\sim$ 1.9 to $\sim$ 2.3 after

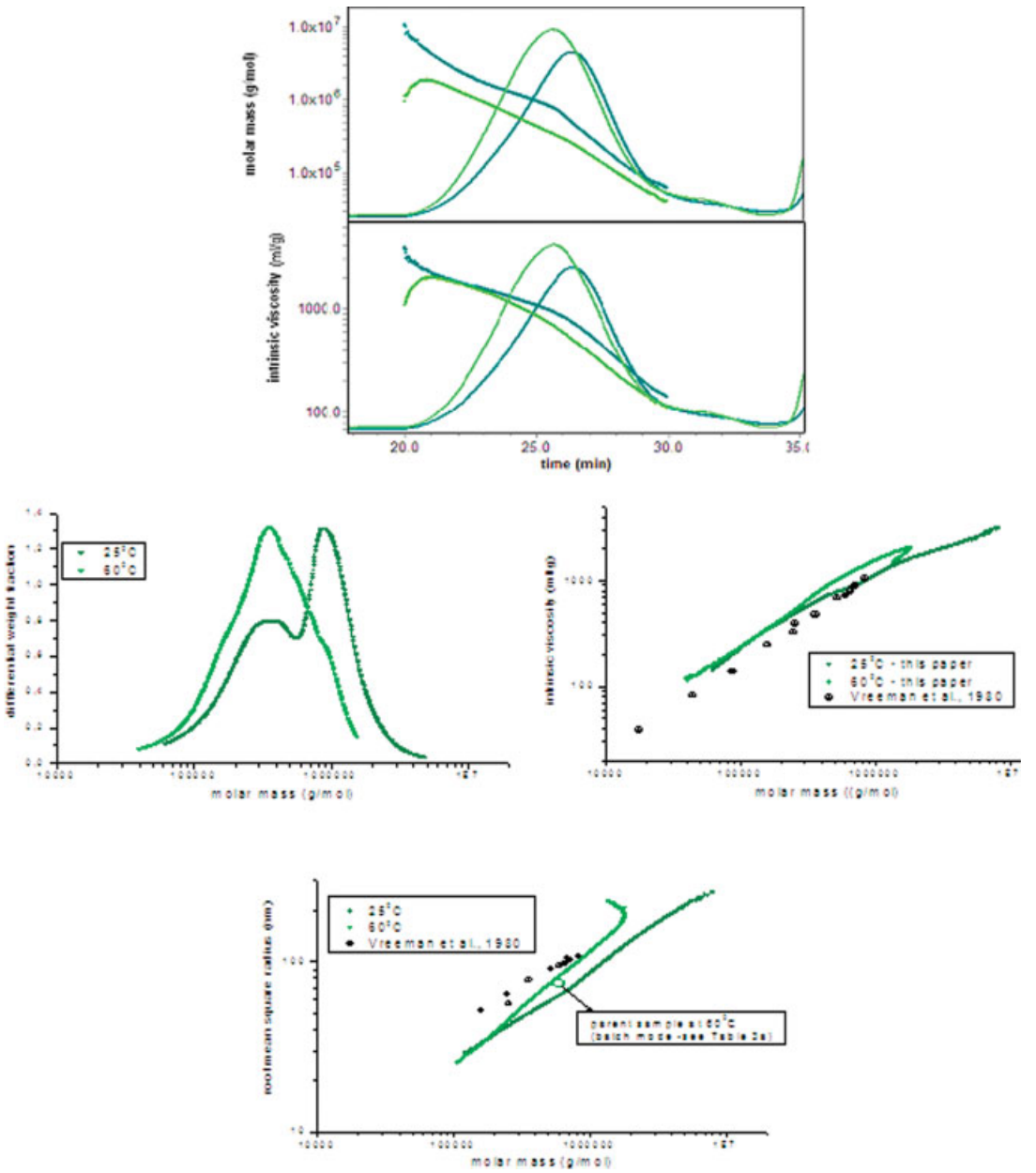

Figure 9 Comparison of kappa-carrageenan at 25°C (dark-green circles) and 60°C (light-green circles). Top: molar mass and refractive index trace versus elution time and intrinsic viscosity and refractive index trace versus elution time. Middle and bottom: differential molar mass distribution followed by Mark-Houwink type plots: [η] versus M_w and "conformation plot." [Color figure can be viewed in the online issue, which is available at www.interscience.wiley.com.]

temperature decline. The increase of M_w for the whole population (Table VIII) amounts to ~ 70% in line with Table IV. $[\eta]_w$ is increased by just 9%.

The [η]-M plot in Figure 8 reveals that neither temperature nor aggregation remarkably modifies the relationship. In contrast, the conformation plot shows a markedly stronger molar mass dependence of the radius at elevated temperature. In both plots, the dark-green curves (25°C) look like having an inflection near $M \approx 7 \times 10^5$ g mol^{-1} as if two somewhat different curves met right here. This may be owed to the poorer separation on the high-molar mass side, so we would not overvalue that phenomenon.

Comparing our results with those in Ref. 1, we find a very fine agreement with respect to $a_{[\eta]} = 0.86$ and $a_R = 0.48$ at room temperature. The position of the lines is shifted along the molar mass axis. Based on their measurements at 20°C in 0.1M NaCl, Vreeman et al.[1] concluded on a partially drained and single-stranded coil-like chain in a thermodynamically good solvent.

TABLE VIII
Comparison of kappa-Carrageenan by HPSEC at Different Temperatures ($\partial n/\partial c$ from Table II and B from Table III)

Temperature (°C)	$\partial n/\partial c$ (mL g^{-1})	$B \times 10^4$ (mL mol g^{-2})	Recovery rate (%)	$[\eta]_w$ (mL g^{-1})	M_w (g mol^{-1})	M_w/M_n
25	0.107	5.470	~ 87	846	762,600	2.262
60	0.127	9.917	~ 88	778	446,100	1.902

Interpretation of data in terms of the wormlike chain model

On the basis of M_w and R_z from the batch mode measurements at 60°C, we were in the position to calculate the characteristic WLC parameters. Therefore, we made use of the Skolnik-Odijk-Fixman approach in the same way as described in detail elsewhere.[20,21] It implies that excluded volume effects may be attributed to solely electrostatic interactions while the contribution of the (hydrophobic) backbone is negligibly small. All formulae may be taken also from Ref. 39, and the temperature-dependent parameters such as the Bjerrum length λ_B and the related Debye length λ_D as well as substance-related parameters such as the mass-per-unit-length M_L are specified in Table IX and footnotes. For the reason of simplicity, we assumed a Schulz-Zimm distribution of the radius for $M_w/M_n = 2.0$ to eliminate polydispersity effects.

For all three samples, we ended up with a nearly uniform intrinsic persistence length $L_{P,i}$ somewhere between 3 and 4 nm and expansion factors α_{exp} as high as 1.5 and above (Table IX). The electrostatic contribution to the persistence length $L_{P,e}$ at the given ionic strength is negligibly small and does not exceed the experimental error. Taking insecurities with regard to the mass-per-unit-length and/or the chemical composition into account, we would estimate our results on kappa-carrageenan in the disordered state to be in good agreement with those by other groups.[1,3] For example, Slootmaekers et al.[3] derived $L_{P,i}$ values of 6.8 or 3.7 nm from light scattering or viscosity measurements. The high expansion factors α_{exp} are consistent with a flexible chain only. The same model applies to all three types of carrageenans in the disordered state in line with the conformation plot and the $[\eta]$-M plot in Figure 7. Following a previous manner of interpretation,[21] we would attribute the relatively high scaling exponents of $a_R = 0.68$ and $a_{[\eta]} \approx 0.8$ to excluded volume and draining effects, respectively.

CONCLUSIONS

The close chemical relationship among the three types of carrageenans has its counterpart in the practically identical WLC characteristics in solution. This could be demonstrated by both batch mode measurements and multidetector HPSEC. Suitable conditions for the macromolecular characterization are a temperature of 60°C and added salt (e.g., $NaNO_3$) equivalent to an ionic strength of 0.1M. The latter has revealed to sufficiently suppress intramolecular charge effects on the conformation as well as electrostatic interactions upon HPSEC. The intrinsic persistence length was calculated to be as small as 3 to 4 nm, which is somewhat lower than what was obtained on chitosans.[21]

Considerably lower or higher ionic strengths are supposed to change that situation. This could be the

TABLE IX
Wormlike-Chain Parameters of Carrageenans at 60°C in 0.1M $NaNO_3$ from Batch Mode Measurements (Table IV)

Sample	M_w (g mol^{-1})	M_0[a] (g mol^{-1})	M_L[a] (g mol nm^{-1})	L_w (nm)	R_z (nm)	R_w[b] (nm)	α_{exp}[c]	$R_{w,\theta}$[d] (nm)	$L_{P,i}$[e] (nm)	$L_{P,e}$[f] (nm)	N_K[g]
κ-carr	596,300	406	406	1469	74.3	60.7	1.58	38.4	3.2	0.17	~ 230
ι-carr	833,600	508	508	1641	86.3	70.5	1.49	47.2	4.1	0.29	~ 200
λ-carr	1,401,000	610	610	2297	93.1	76.0	1.67	45.5	2.7	0.29	~ 425

Calculations performed with Bjerrum length $\lambda_B = 0.76$ nm including $\varepsilon_{water}^{60°C} = 66.82$ and Debye length $\lambda_D = 0.932$ nm.
[a] Mass and length related to the disaccharide repeating unit—sodium salt.
[b] Assuming a Schulz-Zimm distribution of the radius of gyration for $M_w/M_n = 2.0$, which means $r_w \equiv r_z/\sqrt{1.5}$.
[c] Expansion factor to correct for excluded volume effects (based on the Skolnik-Odijk-Fixman (SOF) approach).
[d] Radius of gyration at θ-conditions (unperturbed dimension).
[e] Intrinsic persistence length.
[f] Electrostatic persistence length including ξ_M according to the Manning condensation theory (see, e.g., Ref. 19).
[g] Number of Kuhn segments per chain.

subject of further studies in the context of salt-induced optical activity changes. Better attention than before would have to be paid to the specific refractive index increment and its variation upon various solvent composition and different temperature. Several previously reported results might then appear in the need of revision.

All three types of carrageenans follow the known pattern of behavior in dilute solution showing a differently pronounced tendency for aggregation at room temperature. The "molecular characteristics" of the formed aggregates resembles that of individual molecules. Neither static light scattering nor viscosity has revealed to be useful to distinguish the one sort of species from the other. The sophisticated interpretation of the concentration-dependent angular dependencies upon aggregation at 25°C by master curves[20,46] would certainly lead to a better understanding of the aggregation mechanism and supplement the existing approaches,[16,17] which are based on the concentration dependence of the apparent average molar mass only.

Batch mode and HPSEC on-line MALS have been shown to complement each other. The quality of SEC separation has been shown to strongly affect all kinds of derivable Mark-Houwink type plots. Carefully chosen SEC conditions beside parallel measurements on isolated sample series of graduated molar mass and known polydispersity would help to reduce the risk of misinterpretation.

Once established, a specifically adapted HPSEC approach might ensure quick and safe access to the molar mass distribution as a matter of routine checkups in industry according to the European Commission requirements.[47]

The methodological aspects discussed in the context of the (multi-angle batch mode) static light scattering as well as triple-detector HPSEC apply to any linear polymer.

GB thanks Dr. Philip Wyatt from Wyatt Technology Corporation (Santa Barbara, California, USA) for the opportunity to perform big parts of the presented experimental work in his laboratory. Special thanks are addressed to Dr. David Myslabodski (WTC) for his substantial contribution in planning and doing the experiments. Dr. Shawn Cao (application scientist at WTC) is gratefully acknowledged for technical support.

References

1. Vreeman, H. J.; Snoeren, T. H. M.; Payens, T. A. J. Biopolymers 1980, 19, 1357.
2. Smidsrød, O.; Grasdalen, H. Hydrobiologia 1984, 116/117, 178.
3. Slootmaekers, D.; De Jongh, C., Reynaers, H.; Varkevisser, F. A.; Bloys van Treslong, C. J. Int J Biol Macromol 1988, 10, 160.
4. Norton, I. T.; Goodall, D. M.; Morris, E. R.; Rees, D. A. J Chem Soc Faraday Trans 1983, 79, 2475.
5. Semenova, M. G.; Plashchina, I. G.; Braudo, E. E.; Tolstoguzov, V. B. Carbohydr Polym 1988, 9, 133.
6. Slootmaekers, D.; Mandel, M.; Reynaers, H. Int J Biol Macromol 1991, 3, 17.
7. Slootmaekers, D.; van Dijk, J. A. P. P.; Varkevisser, F. A.; Bloys van Treslong, C. J.; Reynaers, H. Biophys Chem 1991, 41, 51.
8. Vanneste, K.; Slootmaekers, D.; Reynaers, H. Food Hydrocolloids 1996, 10, 99.
9. Wittgren, B.; Borgström, J.; Piculell, L.; Wahlund, H.-G. Biopolymers 1998, 45, 85.
10. Ueda, K.; Itoh, M.; Matsuzaki, Y.; Ochia, H.; Imamura, A. Macromolecules 1998, 31, 675.
11. Bongaerts, K.; Reynaers, H.; Zanetti, F.; Paoletti, S. Macromolecules 1999, 32, 675.
12. Hjerde, T.; Smidsrød, O.; Christensen, B. E. Biopolymers 1999, 49, 71.
13. Viebke, C.; Williams, P. A. Food Hydrocolloids 2000, 14, 265.
14. Bongaerts, K.; Paoletti, S.; Denef, B.; Vanneste, K.; Cuppo, F.; Reynaers, H. Macromolecules 2000, 33, 8709.
15. Meunier, V.; Nicolai, T.; Durand, D. Macromolecules 2000, 33, 2497.
16. Reynaers, H. Fibers Text Eastern Eur 2003, 11, 88.
17. Cuppo, R.; Reynaers, H.; Paoletti, S. Macromolecules 2002, 35, 539.
18. Nickerson, M. T.; Paulson, A. T.; Halett, F. R. Carbohydr Polym 2004, 58, 25.
19. Marcelo, G.; Saiz, E.; Tarazona, M. P. Biophys Chem 2005, 113, 201.
20. Berth, G.; Dautzenberg, H. Recent Res Dev Macromol Res 1998, 3, 225.
21. Berth, G.; Cölfen, H.; Dautzenberg, H. Prog Colloid Polym Sci 2002, 119, 50.
22. Myslabodski, D. E.; Stancioff, D.; Heckert, R. Carbohydr Polym 1996, 31, 83.
23. Utiyama, H. In Light Scattering from Polymer Solutions; Huglin, M. B., Ed.; Academic Press: London, 1972; p 61.
24. Schulz, G. V.; Lechner, M. In Light Scattering from Polymer Solutions; Huglin, M. B., Ed.; Academic Press: London, 1972; p 503.
25. Basedow, M.; Ebert, K. H.; Ruland, U. Makromol Chem 1978, 179, 1351.
26. Huglin, M. B. In Light Scattering from Polymer Solutions; Huglin, M. B., Ed.; Academic Press: London, 1972.
27. Hammel, G. L.; Schulz, G. V.; Lechner, M. D. Eur Polym J 1979, 15, 209.
28. Brandrup, J.; Immergut, E. H.; Grulke, E. A. Polymer Handbook, 4th ed.; Wiley: New York, 1999.
29. Wohlfarth, Ch.; Wohlfarth, B. Landolt Börnstein; Springer: Berlin, 1996.
30. Berth, G.; Dautzenberg, H.; Rother, G. Carbohydr Polym 1994, 25, 177 and 187.
31. Berth, G.; Dautzenberg, H.; Hartmann, J. Carbohydr Polym 1994, 25, 197.
32. Berth, G.; Dautzenberg, H.; Christensen, B. E.; Harding, S. E.; Rother, G.; Smidsrød, O. Macromolecules 1996, 29, 3491.
33. Harding, S. E.; Day, K.; Dhami, R.; Lowe, P. M. Carbohydr Polym 1997, 32, 81.
34. Rollings, J. E. In Laser Light Scattering in Biochemistry; Harding, S. E.; Satelle, D. B.; Bloomfield, V. A., Eds.; Royal Society of Chemistry, 1992; p 275.
35. Wyatt Technology Corporation. Application Note 3/1/96: Irradiation on Sodium Alginate; Wyatt Technology Corporation: Santa Barbara, CA, 1996.
36. Beri, G. B.; Walker, J.; Reese, E. T.; Rollings, J. E. Carbohydr Res 1993, 238, 11.
37. Tanford, Ch. Physical Chemistry of Macromolecules, 3rd ed.; Wiley: New York, 1965.
38. Girod, S.; Baldet-Dupy, P.; Maillols, H.; Devoiselle, J.-M. J Chromatogr A 2001, 943, 147.
39. Dautzenberg, H.; Jaeger, W.; Kötz, J.; Philipp, B.; Stscherbina, D. Polyelectrolytes—Formation, Characterization and Application; Hanser Publishers: Munich, 1994.

40. Marinalg International. Marinalg International Position Paper regarding European Union: Molecular Weight Specification for Carrageenan (E407), January 2007.
41. Wyatt, P. In Laser Light Scattering in Biochemistry; Harding, S. E.; Satelle, D. B.; Bloomfield, V. A., Eds.; Redwood Press Ltd.: Melksham, Wiltshire, UK, 1992; p 35.
42. Marheineke, N. LC GC Europe 2005, 18, 17. Viscotek—Applications-Book; 2005; Vol. 17, p 2.
43. Yamakawa, H. Modern Theory of Polymer Solutions; Harper and Row: New York, 1971.
44. Grubisic, Z.; Rempp, P.; Benoit, H. Polym Lett 1967, 5, 753.
45. Uno, Y.; Omoto, T.; Goto, Y.; Asai, I.; Nakamura, M.; Maitani, T. Food Additives Contaminants 2001, 18, 763.
46. Dautzenberg, H.; Rother, G. J Polym Sci Part B: Polym Phys 1988, 26, 353.
47. European Commission. Opinion of the Scientific Committee on Food on Carrageenan, SCF/CS/ADD/EMU/199 Final, http://ec.europa.eu/food/fs/sc/scf/out164_en.pdf, February 21, 2003.